Low-symmetry phases and loss of relaxation in nanosized lead scandium niobate

J. M. Kiat,[1,2] C. Bogicevic,[1] F. Karolak,[1] G. Dezanneau,[1] N. Guiblin,[1] W. Ren,[3] L. Bellaiche,[3] and R. Haumont[4]
[1]*Laboratoire Structures, Propriétés et Modélisation des Solides, CNRS-UMR8580, Ecole Centrale Paris, Grande Voie des Vignes, 92295 Châtenay-Malabry Cedex, France*
[2]*Laboratoire Léon Brillouin, CNRS-UMR12, CE Saclay, 91991 Gif-Sur-Yvette Cedex, France*
[3]*Department of Physics, University of Arkansas, Fayetteville, Arkansas 72701, USA*
[4]*Laboratoire de Physico-Chimie de l'Etat Solide, ICMMO, CNRS-UMR8182, Université Paris XI, 91405 Orsay, France*
(Received 25 November 2009; published 23 April 2010)

Using a combination of experimental and theoretical techniques, we reveal that lead scandium niobate (PSN) nanograins exhibit a critical size of ≈65 nm below which the ground state is not anymore rhombohedral but rather monoclinic for chemically disordered systems. A triclinic ground state is further found for chemically ordered nanosized PSN. Such changes in symmetry are associated with a change in the polarization's direction, as well as, with an enhancement of the polarization's magnitude and a vanishing of relaxation. First-principles-based calculations point toward an internal electric field and mechanical constraints for the origins of these unexpected features.

DOI: 10.1103/PhysRevB.81.144122 PACS number(s): 77.84.Ek, 64.70.Nd, 77.80.−e, 81.07.Wx

I. INTRODUCTION

The so-called "*relaxor*" compounds exhibit a strong, anomalous dependency of their dielectric response with frequency, making them fundamentally intriguing [see Refs. 1 and 2, and references therein]. Moreover, the bulk solid solutions formed by the alloying of Pb-based relaxors with lead titanate $PbTiO_3$ (PT) display a huge enhancement of their properties (which makes them suitable for a variety of applications), when the Ti concentrations are in the narrow range defining the "*morphotropic phase boundary*" (MPB). Such huge enhancement typically originates from the existence of monoclinic phases in which the polarization is allowed to freely rotate[3–6] in a plane (contrarily to usual ferroelectrics with axial polar phases) in this MPB area.

One may wonder what happens to properties of *low-dimensional* Pb-based relaxors, and how their sizes affect their ground states, keeping in mind this strong relationship evidenced also when alloying with PT; for instance, the recent report (and controversies) on PZN relaxors (e.g., Ref. 7) shows the existence of two different structures related to the surface and core. Motivated to resolve such important issues, we decided to experimentally and theoretically study nanosized lead scandium niobate $PbSc_{1/2}Nb_{1/2}O_3$ (PSN).

PSN is particularly attractive because (in its bulk form): (1) contrarily to other relaxors such as $PbMg_{1/3}Nb_{2/3}O_3$ (PMN), for which no long-range polar order emerges, PSN spontaneously transforms into a rhombohedral ferroelectric phase[8] and (2) because of its high-temperature order-disorder transformation (1210 °C), which allows to control the local degree of ordering of Sc and Nb by very long-time thermal annealing, drastic changes in properties result.[8,9]

In this paper, we show, by combining experimental and theoretical approaches, that the long-range rhombohedral axial polarization of PSN jumps toward a low monoclinic symmetry's direction, below a nanometric critical size for chemically *disordered* systems—while nanosized *ordered* PSN exhibits a triclinic ground state. Such jump is accompanied by an enhancement of the polarization's magnitude and a vanishing of relaxation (exactly as in lead-based solid solutions near their MPB). First-principles-based calculations indicate that such unusual features stem from the existence of internal electric fields coupled with mechanical constraints.

II. METHODS

A. Experiment

In order to carefully check the consistency of our experimental data, we have synthesized nanopowders using *three* different routes that are described in detail elsewhere:[10,11] (i) the *classical two-step Wolframite route* which gives micrometric samples being afterward grinded to reach a 20 nm grain size; (ii) the *mechanical activation* in which the solid-state reaction with the starting oxides is activated by mechanical energy rather than temperature; (iii) the *freeze-drying method* in which a precursor solution is nozzle sprayed into liquid nitrogen, the solvents being eliminated by sublimation from the resulting frozen droplets which are afterward calcinated. Nanopowders with grain size ranging from 20 nm to 1 μm were prepared by annealing the as-prepared nanometric powders at different temperatures. Special attention was paid to avoid undesirable strain by further heat treatments. As-prepared samples are chemically *disordered*, as classically[9] indicated by the absence of superstructure peaks. Very long-time annealing (typically 1 month at 1000 °C) of a micrometric *disordered* sample was needed to obtain a micrometric *ordered* sample, as evidenced by the presence of superstructure peaks. A part of this powder was subsequently grinded (typically 24 h) to obtain a 20 nm chemically *ordered* sample of PSN.

Low- and high-temperature x-ray diffraction patterns were collected on a highly accurate two-axis diffractometer with rotating anode generator. The *R*-expected agreement factor (which is a measure of the statistic quality) were typically around 2.8%, which is rather satisfactory for Rietveld refinements. We have used the standard methodology for the Rietveld analysis of relaxors and MPB compounds, as in our

previous works (see, e.g., Refs 4–6, 9, and 10); as well known, this method uses the full pattern of diffraction to refine a given structural model. In particular, we have tested many single-phase models, among them the $R3m$, Cm, Pm, $P1$, $P4mm$, $Amm2$, and $Pm\bar{3}m$ space groups, and their phase mixings, which are observed in the MPB compounds studies. The small number of independent oxygen atoms (i.e., 1 for $R3m$, 2 for Cm, and 3 for Pm and $P1$ space groups) to be refined and in addition the fact that not all x, y, and z coordinates have to be refined (in total only 1 coordinate for $R3m$, 5 for Cm, 6 for Pm, and 7 for the $P1$ cases since many of them are on special positions) allowed us to determine the oxygen atoms. Note also that the resulting ground state for a given grain size was systematically found to be independent of the used chemical route.

Variation in dielectric permittivity has been measured with an impedance analyzer (Hewlett Packard 4192A) with a cryofurnace between 100 and 450 K and between 1 and 100 kHz, with a heating and cooling rate of 3 °C/min. We have measured the dielectric properties of powders as well as of ceramics with decreasing submicron grain sizes. The samples used for these measurements were the same powders used for the x-ray diffraction. In this purpose, we have made a simple densification with a press at room temperature, and have heated the pastilles at 400 °C for 1 h in order to realize possible induced internal strain. This process allowed avoiding grain growth (as checked by using x-ray diffraction and electron microscopy). In some case, we also make ceramics by hot pressing, which gave samples in the high grain-size range, in order to check that the results are the same as in the pastilles. We have measured that the density typically ranges between 98% and 88%, and have performed extensive scanning electron microscopy, transmission electron microscope, atomic force microscopy, and x-ray characterizations. In each case, we have chosen the best samples for the dielectric measurements and make comparison for given grain sizes of the results to ensure a good reproducibility. The data have been corrected using the Rushman and Striven equation, as classically done, which gave, in this case, equivalent results to a simple normalization by the relative density.

B. Computation

Regarding computations, we used a first-principles-derived effective Hamiltonian to mimic PSN nanodots,[12] as represented by $n \times n \times n$ supercells. Its degrees of freedom are the local soft-mode amplitudes in each five-atom unit cell (which are directly proportional to the local electric dipoles centered in these cells) and the strain tensor (that contains both homogeneous and inhomogeneous parts). The chemical configuration between Nb and Sc atoms in the $n \times n \times n$ supercells is chosen at the beginning of the simulations and kept frozen during these simulations.

As in Ref. 12, the total internal energy of the effective Hamiltonian has two main terms. The analytical expression and parameters of the first energetic term are those of Ref. 13 for *bulk* PSN (which lead to the correct phase-transition sequence from a cubic paraelectric state to a rhombohedral ferroelectric state as the temperature decreases), except for the dipole-dipole interaction for which the self-consistent formula derived in Ref. 12 for dots under open-circuit (OC) conditions is used (note that our model also assumes a truncation, at the surface layers, of the interactions existing in bulk PSN). The second energetic term allows a screening of the magnitude of the maximum depolarizing field (associated with OC conditions and with a nonzero polarization) via a β parameter: $\beta=0$ corresponds to OC conditions (no screening of the maximum depolarizing field) while an increase in β lowers the magnitude of the residual depolarizing field, and $\beta=1$ corresponds to ideal short-circuit conditions (for which the depolarizing field has vanished). Note that Ref. 12 found that the ground state of stress-free ferroelectric nanodots consists of a vortex structure that does not exhibit any polarization (but rather an electric toroidal moment) and that is mostly independent of β, when β is smaller than 0.95, in order to completely annihilate the depolarizing field. On the other hand, such nanodots possess a polarization whose magnitude strongly depends on β (as well as on the dots' size) when β is larger than 0.95, as a result of the fact that the depolarizing field increases in magnitude (and thus more strongly fights against the polarization) as β is decreased from 1 to 0.95. Here, we constantly chose a β parameter equal to 0.97 because such value has been found to accurately reproduce various experiments[14] on different ferroelectric nanostructures. All the parameters entering the total energy of this effective Hamiltonian are determined from first principles,[13] and this energy is used into Monte Carlo simulations to obtain finite-temperature properties of PSN nanodots. Note that effective Hamiltonian approaches have been previously shown to accurately reproduce many striking features of ferroelectric nanostructures, (see, e.g., Ref. 15).

III. RESULTS

A. X-ray study of ground states

At low temperature (85 K), in a grain-size range of 65 nm and higher, using the Rietveld analysis yields the classical ground state already reported by several authors,[5,6,8,9] that is the ferroelectric axial rhombohedral $R3m$ phase (which is observed in disordered or ordered sample). On the other hand, *disordered* samples with a grain size smaller than the "critical" value of $r_c \approx 65$ nm are no more rhombohedral but rather display a ferroelectric monoclinic ground state Pm (M_C in the notation of Ref. 16). Indeed, in these cases, a much better agreement (as defined in particular by the R_B factor that is proportional to the difference between diffraction intensities calculated from the structural model used in the Rietveld analysis and experimental data) is obtained for the Pm monoclinic model among all structural models we have tested, leading to a better matching between the observed and calculated profiles. For instance, R_B is equal to 5.69% in the $R3m$ model versus 3.91% in the Pm model for 20 nm samples, and improvement as large as typically 1.5% to more than 2% were systematically observed, demonstrating the occurrence of the Pm structure at low grain size. This is evidenced by Fig. 1 in which three peaks with simple Millers indices, extracted from the full experimental and cal-

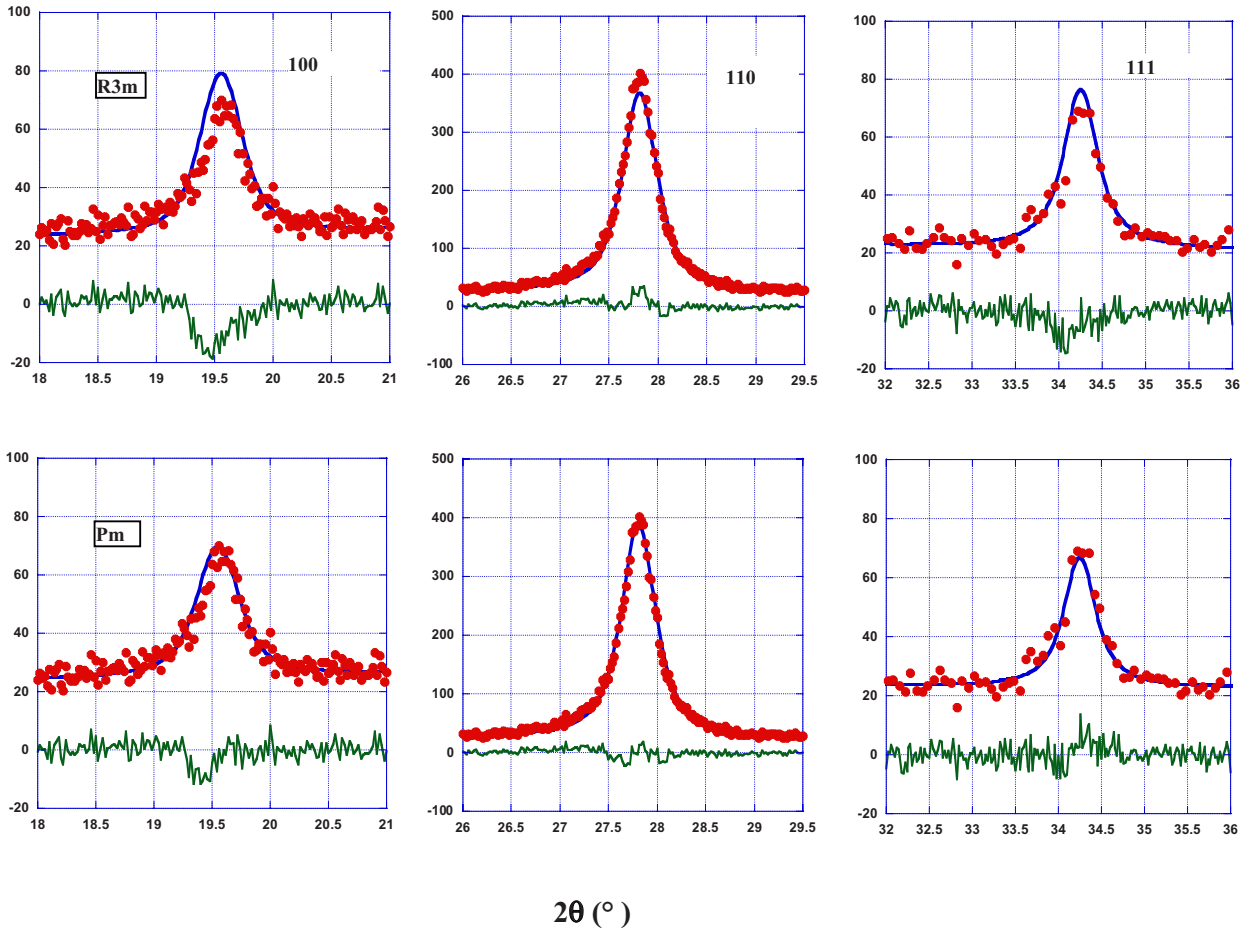

FIG. 1. (Color online) Three characteristic Bragg peaks for a 20 nm chemically disordered sample. The red dots represent the actual data, 2 theta/intensity in arbitrary unit while the blue and green lines display the fit by a structural model and the difference between the actual data and such fit, respectively. The structural model is a *R*3*m* (respectively, *Pm*) state in the top (respectively, bottom) row.

culated patterns, are shown. This *Pm* phase coexists with a very small (on the order of a few percent), size-dependent amount of the rhombohedral phase, as reported in the right part of Fig. 2 (blue diamond). This amount changes abruptly above $r_c \approx 65$ nm: as a matter of fact, only the *R*3*m* phase is observed when $r > r_c$.

A very surprising result was obtained in the case of the 20 nm *ordered* sample: we have not observed the *Pm* monoclinic phase (nor the *R*3*m* phase) but rather a *triclinic* *P*1 phase. Indeed, much better R_B were obtained with this *P*1 phase (3.72%) than in the case of a mixing of majority *Pm* monoclinic with rhombohedral phases (4.64%) while the quality of the fitting by a sole *R*3*m* phase was rather poor (9%).

At high temperature, all *disordered* or *ordered* sample, independently of their grain size, exhibit the well-known $Pm\bar{3}m$ cubic paraelectric phase. Samples with $r > r_c$ transform from the *R*3*m* ferroelectric phase into the cubic paraelectric phase whereas samples with $r < r_c$ transform from the *Pm* monoclinic or *P*1 ferroelectric phase into the cubic paraelectric phase. In the latter case, this is a situation exactly found in MPB bulks. However in our case, the precise value of the critical temperature is difficult to experimentally determine in samples with low grain sizes, due to large widening of Bragg peaks, and requires full patterns recordings and refinements at every temperature.

Following the pioneering work by Hewat[17] which has been extensively used in structural studies of relaxors and MPB compounds, we have used the atomic positions obtained in the Rietveld analysis and the effective charges given by this author in order to calculate the magnitude and orientation of the polarization within the structures. The left part of Fig. 2 reports the magnitude of the polarization (red dots and square) versus grain size: when the grain size becomes smaller this magnitude does not strongly diminish in the rhombohedral phase (that is in the $r > r_c$ range). On the other hand, a drastic enhancement (factor ≈ 2) of the polarization's magnitude is observed as the size decreases in the monoclinic phase of nanosized PSN (that is in the $r < r_c$ range). For the 20 nm *ordered* sample, the *P*1 polarization becomes even stronger, almost two times larger, than that of the *Pm* phase occurring in $r \leq r_c$ disordered samples and ≈ 3 times larger than that of the *R*3*m* phase associated with $r > r_c$ disordered samples.

Regarding the direction of the polarization of the *disordered* samples, the fact that the *Pm* monoclinic plane containing the polarization does *not* possess any rhombohedral ⟨111⟩ direction automatically implies that the size-induced jump of the polarization's direction from a rhombohedral

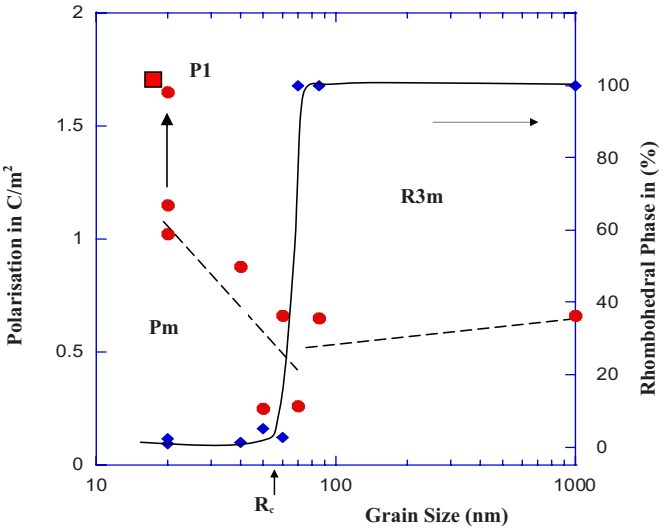

FIG. 2. (Color online) Right: percentage of rhombohedral phase at 85 K (blue diamond). Left: magnitude of the polarization (red dots and square), as calculated from structural refinements and effective charge of ions. All samples are chemically *disordered* (red dots) except one (red square) that is chemically *ordered* with a characteristic grain size of 20 nm (and that adopts the *P*1 symmetry).

⟨111⟩ direction toward a monoclinic *Pm* ⟨*uv*0⟩ direction is discontinuous in nature (such as in MPB systems). We have observed that at low temperature, all the $r \leq r_c$ samples have a polarization pointing along a ⟨*uv*0⟩ direction, with *u* larger than *v*. At low temperature, the polarization is therefore close to, but definitively deviates from, a tetragonal ⟨100⟩ direction (the angle formed by the polarization and this ⟨100⟩ pseudocubic direction is typically between 5° and 10°).

B. Dielectric studies of the relaxation

The temperature and frequency dependence of the real permittivity have been examined for each sample. In the case of high grain sizes, we obtained the classical evolution already reported[8,9] and that is characterized by a strong anomaly in a large temperature range with high-frequency relaxation, i.e., a change in the temperature at which the dielectric response is maximum with the applied frequency. When reducing the grain size, the temperature at which the permittivity is maximum, T_{max}, strongly increases, changing from 360 to 422 K whereas the maximum value of the dielectric constant, ε_{max}, strongly decreases from more than 14 000 to less than 300 with an associated strong increase in diffusivity (Figs. 3 and 4). The magnitude of the relaxation, which can be characterized by T_{max}(1 MHz)-T_{max}(1 KHz), also decreases with the grain size. Moreover, for grain sizes below and close to r_c, the frequency relaxation does not follow the well-known Vögel Fulcher law of relaxors (such law is observed above r_c). In fact, such relaxation vanishes at the lowest grain sizes (see inset of Fig. 4). All these behaviors bear resemblance with those observed in nanosized PMN.[10,18]

C. Effective Hamiltonian simulations

In order to gain insight into all the intriguing, experimental results summarized in Figs. 1–4, we now turn our attention to the predictions from the effective Hamiltonian approach described in Sec. II B. Figure 5(a) and its top inset report the Cartesian components (u_x, u_y, u_z) of the local mode—which is directly proportional to the polarization[13]—in *stress-free disordered* PSN nanodots having 4.8 nm and 4.0 nm lateral size, respectively—with *x*, *y*, and *z* axes being along the pseudocubic [001], [010], and [001] directions. (Here, the disordered atomic configuration is generated by a random algorithm for each dot's size and is kept fixed during the simulations.) The bottom inset of Fig. 5(a) displays the *magnitude* of such polarizations versus temperature. One can clearly see that (i) the polarization in the ground state deviates from a ⟨111⟩ direction in these nanometric dots (since u_x, u_y, and u_z are all different from each other and nonzero at low temperature); (ii) this deviation typically increases, as the size of the stress-free disordered dot decreases; (iii) the polarization of the ground state increases in magnitude when shrinking the dots; and (iv) the paraelectric-to-ferroelectric transition is more diffuse as the dots become smaller. Such features are found to all originate

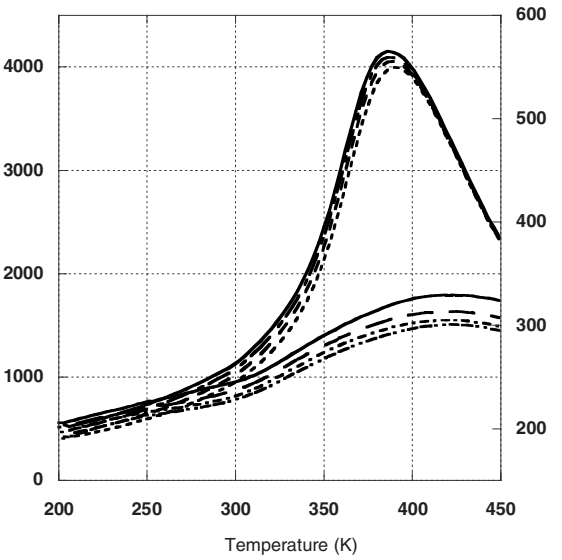

FIG. 3. Temperature evolution of real permittivity for $r > r_c$ (95 nm) and $r < r_c$ (40 nm) grain size at 1, 10, 100, and 1 MHz.

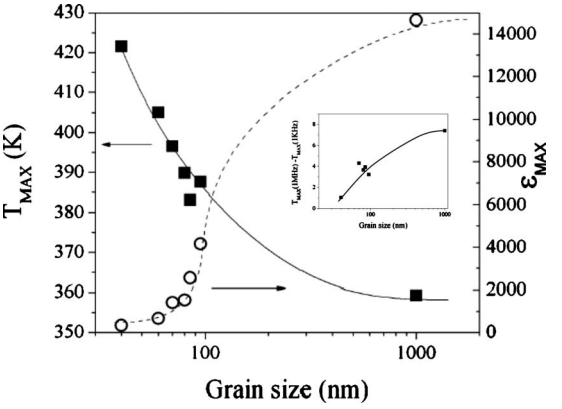

FIG. 4. Grain-size dependency of T_{max} and ε_{max}. The inset displays T_{max}(1 MHz)-T_{max}(1 KHz) versus the grain size.

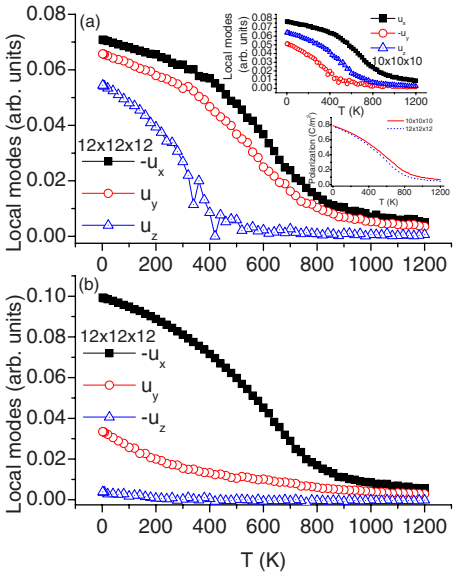

FIG. 5. (Color online) Cartesian components of the local mode versus temperature in a disordered $12\times12\times12$ PSN nanodot (i.e., with a lateral size of 4.8 nm) for stress-free conditions [panel (a)] and under a biaxial stress of −3 GPa in the (y,z) plane [panel (b)]. The top inset of panel (a) shows such Cartesian components for a stress-free disordered $10\times10\times10$ PSN nanodot (lateral size of 4 nm) while its bottom inset displays the magnitude of the polarization in these stress-free $12\times12\times12$ and $10\times10\times10$ dots. Negative sign in front of u_x, u_y, or u_z indicates that such component is negative. We numerically found that u_α (with α=x, y, or z) is negative (respectively, positive) if the internal field caused by the atomic arrangement between Sc and Nb ions has a negative (respectively, positive) component along the α axis.

from the internal electric field generated by the fact that Sc and Nb atoms belong to different columns of the periodic table.[19] Interestingly, unlike in the disordered PSN bulk for which the internal field resulting from Sc and Nb distributions has a null value when averaged over the whole sample,[19] the internal field in the PSN dots is numerically found to have a definite *nonzero* spatial averaged value—which is mostly due to the existence of surfaces. In other words, the nanoscale disordered PSN dots can be thought as being under the influence of a dc electric field. Moreover, decreasing the size of the disordered dot is numerically found to have two important consequences on such electric field: it increases its magnitude [therefore explaining items (iii) and (iv)], and it makes such field more anisotropic [which explains items (i) and (ii)]. Note that items (i), (iii), and (iv) *are fully consistent with our measurements described above*. Moreover, it is known that applying a dc electric field in relaxors (bulks) leads to a decrease in relaxation and ultimately reinstates a ferroelectric state.[20] The internal electric field discovered by our simulations, and its size dependency aforementioned, therefore also explains the size-induced decrease and then disappearance of relaxation experimentally seen in our smallest nanosized PSN samples. (Note that the theoretical transition temperatures are larger than the experimental ones likely because the simulated dots are much smaller in size than those grown, as consistent with Fig. 4.) On the other hand, the predicted polarization in the stress-free dots is not necessarily found to be along a $\langle uv0\rangle$ direction at low temperature (or equivalently, the simulated ground state is not always a *Pm* phase). For instance, Fig. 5(a) points toward a monoclinic *Cm* phase with a polarization along $\langle uuv\rangle$ in the $12\times12\times12$ nanodot while its top inset reports a triclinic state with the polarization being parallel to $\langle uvw\rangle$ in the $10\times10\times10$ nanodot (these different polarizations and associated ground states result from the anisotropy between the Cartesian components of the internal electric field). In fact, we numerically found that systematically obtaining a *Pm* state with a polarization lying along a $\langle uv0\rangle$ direction in the disordered PSN nanodots requires *mechanical* constraints, in addition to the existence of the internal electric fields. As a matter of fact and as shown in Fig. 5(b), applying a biaxial stress in the (y,z) plane does lead to the monoclinic *Pm* ground state and to the polarization's direction measured in chemically disordered nanosized PSN. Similarly, applying some shear stresses to *ordered* PSN nanodots (for which no internal electric fields exist because of the perfect atomic ordering[19]) generate the ground state that we experimentally observed, that is of triclinic symmetry. Note that long-time grinding (that was necessary to experimentally obtain the ordered sample) is known to generate shear stresses.[21]

IV. SUMMARY AND DISCUSSION

In fine, this study of PSN, which is an axial ferroelectric rhombohedral relaxor at bulk micrometric sizes, has revealed deep changes in its structural behavior and physical properties at nanometric sizes. Indeed, using a combination of experimental and theoretical techniques, we have observed below a critical size of ≈65 nm a ground state that is not anymore rhombohedral (i.e., that does not have an uniaxial polarization) but rather becomes monoclinic (i.e., that exhibits a planar polarization), for chemically disordered compounds. Long-time annealing and grinding allowed us to prepare ordered nanosized PSN that surprisingly possesses a triclinic ferroelectric ground state.

These monoclinic and triclinic low symmetries are rather unexpected since they are not observed in micrometric relaxors (such as PSN or PMN).[1,3–5] On the other hand, they are usually observed in the MPB of solid solutions formed by the alloying of relaxors with PT. Such low-symmetry states are accompanied by an enhancement of the polarization's magnitude and a vanishing of relaxation in PSN nanodots, as, once again, found in MPB bulk systems.

Our first-principles-based calculations have been able to reproduce various effects of reduction in grain sizes, e.g., the deviation of the polarization's direction from a $\langle111\rangle$ axis, and the enhancement of the magnitude of polarization, and the increase in diffusivity as the nanodot's size decrease. Moreover, they have given some clues for the origin of these unexpected features. Indeed, two important components in the calculation were evidenced in order to reproduce and understand all experimental effects: (i) first of all, strong internal electric fields resulting from the Sc/Nb atomic occupations and the existence of surfaces and (ii) second,

mechanical constraints introduced in the form of biaxial or shear stresses.

Ultimately, as a nonrelaxor state, as well as, low-symmetry ground states with huge polarization were observed in (lead-titanate-free) PSN, the present study strongly suggests that a global mechanism solely based on the competition between internal elastic and electric fields and the size of the system is likely responsible for the properties of relaxors and MPB compounds.

ACKNOWLEDGMENTS

L.B. acknowledges NSF Grants No. DMR-0701558 and No. DMR-0080054 (C-SPIN), ONR Grants No. N00014-04-1-0413, No. N00014-08-1-0915, and No. N00014-07-1-0825, and DOE Grant No. DE-SC0002220. Some computations were made possible thanks to the MRI NSF Grant No. 0722625 and to a Challenge grant from HPCMO of the U.S. Department of Defense.

[1] J. M. Kiat and B. Dkhil, *Advanced Dielectric, Piezoelectric and Ferroelectric Materials: Synthesis, Properties and Applications*, edited by Z. G. Ye (Woodhead, Cambridge, England, 2007), p. 391.

[2] B. P. Burton, E. Cockayne, S. Tinte, and U. V. Waghmare, Phase Transitions **79**, 91 (2006).

[3] B. Noheda and D. E. Cox, Phase Transitions **79**, 5 (2006).

[4] J. M. Kiat, Y. Uesu, B. Dkhil, M. Matsuda, C. Malibert, and G. Calvarin, Phys. Rev. B **65**, 064106 (2002).

[5] R. Haumont, B. Dkhil, J. M. Kiat, A. Al-Barakaty, H. Dammak, and L. Bellaiche, Phys. Rev. B **68**, 014114 (2003).

[6] R. Haumont, A. Al-Barakaty, B. Dkhil, J. M. Kiat, and L. Bellaiche, Phys. Rev. B **71**, 104106 (2005).

[7] G. Xu, Z. Zhong, Y. Bing, Z.-G. Ye, C. Stock, and G. Shirane, Phys. Rev. B **70**, 064107 (2004).

[8] F. Chu, I. M. Reaney, and N. Setter, J. Appl. Phys. **77**, 1671 (1995).

[9] C. Malibert, B. Dkhil, J.-M. Kiat, J.-F. Bérar, and A. Spasojevic-de Biré, J. Phys.: Condens. Matter **9**, 7485 (1997).

[10] J. Carreaud, P. Geimeiner, J. M. Kiat, B. Dkhil, C. Bogicevic, T. Rojac, and B. Malic, Phys. Rev. B **72**, 174115 (2005).

[11] C. Bogicevic, F. Lacour, C. Malibert, B. Dkhil, C. Ménoret, H. Dammak, M. L. Giorgi, and J. M. Kiat, Ferroelectrics **270**, 57 (2002).

[12] I. Ponomareva, I. I. Naumov, I. Kornev, H. Fu, and L. Bellaiche, Phys. Rev. B **72**, 140102(R) (2005).

[13] R. Hemphill, L. Bellaiche, A. Garcia, and D. Vanderbilt, Appl. Phys. Lett. **77**, 3642 (2000).

[14] L. Louis, P. Gemeinert, I. Ponomareva, L. Bellaiche, G. Geneste, W. Ma, N. Setter, and B. Dkhil, Nano Lett. **10**, 1177 (2010).

[15] I. A. Kornev, B.-K. Lai, I. Naumov, I. Ponomareva, H. Fu, and L. Bellaiche, *Advanced Dielectric, Piezoelectric and Ferroelectric Materials: Synthesis, Properties and Applications*, edited by Z. G. Ye (Woodhead, Cambridge, England, 2007), p. 570.

[16] D. Vanderbilt and M. H. Cohen, Phys. Rev. B **63**, 094108 (2001).

[17] A. W. Hewat, Ferroelectrics **6**, 215 (1974).

[18] J. Carreaud, C. Bogicevic, B. Dkhil, and J. M. Kiat, Appl. Phys. Lett. **92**, 242902 (2008).

[19] J. Iñiguez and L. Bellaiche, Phys. Rev. B **73**, 144109 (2006).

[20] G. A. Samara, J. Phys.: Condens. Matter **15**, R367 (2003).

[21] D. Lewis, D. O. Northnwood, and R. C. Reeve, J. Appl. Crystallogr. **2**, 156 (1969).